

# Pressure Induced *Complexity* in a Lithium Monolayer

A. Rodriguez-Prieto and A. Bergara

*Materia Kondentsatuaren Fisika Saila, Zientzia eta Teknologia Fakultatea,  
Euskal Herriko Unibertsitatea, 644 Postakutxatila, 48080 Bilbo, Basque Country, Spain*

(Dated: November 20, 2018)

Light alkali metals have usually been considered as *simple* metals due to their monovalency and high conductivity. In these metals ionic pseudopotentials are weak and the nearly free electron model (NFE) becomes quite accurate at normal conditions. However, very recent experiments have shown that at high pressures their electronic properties deviate radically from the NFE model and even become unexpected good superconductors. In this work we present *ab initio* calculations to analyze the deviation from simplicity in a lithium monolayer (ML) when pressure is applied. We have seen that as a result of the increasing non-local character of the atomic pseudopotential with increasing pressure, the surprising half filling Hubbard-type nesting observed in the Fermi *line* can explain the interesting *complex* behavior in lithium ML, induced by its correlated structural, electronic and even magnetic properties.

PACS numbers: 71.18.+y, 71.15.Mb, 68.35.-p, 73.20.At

## I. INTRODUCTION

Light alkalies are usually considered as *simple* metals, because as a consequence of the weak interaction between valence electrons and ionic cores, under normal conditions they crystallize in simple high symmetric structures. Therefore, the nearly free electron model (NFE) has been considered a good approximation to describe their electronic properties [1]. The only exception is hydrogen which, even when solidifies, forms very stable diatomic molecules and presents an insulating character. However, recent both theoretical and experimental results have changed our perception of the alkalies and have shown that the NFE model breaks when high pressures are applied. Neaton *et al.* reported *ab initio* calculations for bulk lithium [2] and predicted that pressure could induce structural transitions to less symmetric, lower coordinated structures, associated with electronic localizations. These theoretical predictions have been confirmed by experiments [3], finding that around 40 GPa a phase transition to a complex structure (*cI16*) with 16 atoms per unit cell occurs. It is important to notice that pressure induced transitions from simple to more complex structures are not singular to lithium but have also been predicted in heavier alkalies [4, 5]. On the other hand, other very recent experiments [6, 7, 8] have also shown that at this pressure range lithium presents a superconducting transition with  $T_c \sim 20$ K, becoming the highest transition temperature between simple elements [9]. It is noteworthy that experiments looking for superconductivity in lithium under ambient pressure have failed [10]. This even rises the interest to characterize the physical properties of compressed lithium close to the observed electronic and structural transitions.

In this article we present an *ab initio* theoretical analysis of the pressure-induced structural, electronic and even magnetic properties of a lithium ML. The develop-

ment of new techniques for the atomic manipulation [11, 12] allows the growth of atomic monolayers on inert substratum, semiconductors or noble gases. These new possibilities rise the interest to analyze physical properties of low dimensional systems under different conditions. On the other hand, the simplicity of the atomic configuration associated to the ML facilitates the performing of a more detailed analysis, and extending our conclusions to the bulk will also provide an interesting perspective to understand the physical origin of the experimentally observed features of compressed lithium. In Section II we describe the theoretical and computational background of this work. Results and Conclusions will be presented in Sections III and IV, respectively.

## II. THEORETICAL AND COMPUTATIONAL BACKGROUND

In order to describe structural and electronic properties of a lithium ML over a wide range of densities we have used a plane-wave implementation of the Density Functional Theory (DFT) [13, 14] within the Local Density Approximation (LDA) [15, 16, 17] for non magnetic calculations and Local Spin Density Approximation (LSDA) [18] to analyze the magnetic properties of the ML. All calculations have been performed with the Vienna Ab initio Simulation Package (VASP)[19, 20]. Effects of compression were simulated by reducing the lattice parameter. As the atomic spacing is reduced a significant core overlap is observed, so that we have required methods which take into account core electrons. For fully treating them we make use of the Projector Augmented Wave (PAW) method [21]. A Monkhorst-Pack [22] mesh of  $20 \times 20 \times 1$  has been chosen for the sampling of the Brillouin zone. The description of the ML is implemented by a supercell which, in order to

minimizes interactions between MLs, contains ten layers of vacuum between MLs. The ions are relaxed to their equilibrium positions by calculating the forces acting on them using the Hellmann-Feynmann theorem. In all the calculations we have used an energy cutoff of  $E_{\text{cut}} \simeq 815\text{eV}$ .

### III. RESULTS

#### A. Structural and Electronic Analysis.

Following the analysis in Ref. [23], as a first step we will just consider three simple structures of a lithium ML: hexagonal (*hex*), square (*sq*) and honeycomb (*hc*). Fig. 1 shows the calculated enthalpies for these structures. As it is a common property of the alkalies, lithium ML at equilibrium ( $r_s = 3.02$  a.u.) [24] also favors the compact hexagonal structure (*hex*). However, as we can observe in Fig. 1, at  $r_s < 2.25$  a.u. the more open square structure (*sq*) becomes favored over the hexagonal one.

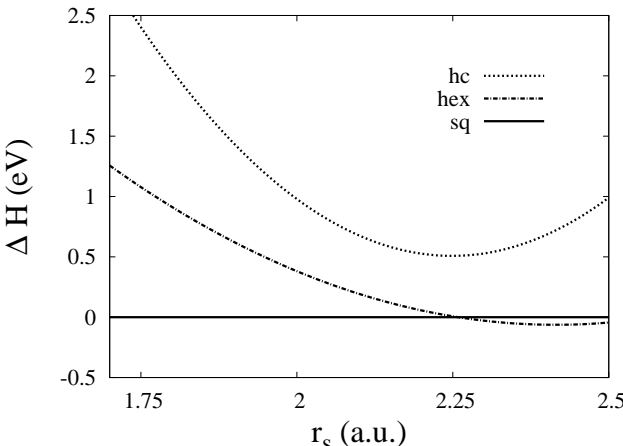


FIG. 1: Enthalpy  $H = E + \sigma A$ ,  $\sigma$  being the surface tension:  $\sigma = -dE/dA$ , as a function of the density parameter,  $r_s$ , for three simple structures: hexagonal (*hex*), square (*sq*) and honeycomb (*hc*). All enthalpies are referenced to the square structure,  $\Delta H = H - H_{\text{sq}}$ .

In Fig. 2 we plot the band structure and density of states (DOS) of a lithium ML corresponding to the hexagonal structure at equilibrium and the square structure with  $r_s = 2.15$  a.u., just after the structural transition. At equilibrium (Fig. 2a) only one band is occupied, which is characterized by a parabolic-type dispersion of  $s$  character, as corresponds to a good NFE-like system. For occupied energies the DOS is almost constant, which reflects the quasi two-dimensional character of the ML. However, at higher pressures (Fig. 2b) the first band flattens associated to the increasing of the band gap at the zone boundary, indicating a clear electronic localization. The energy difference between the first two bands

at  $\Gamma$  decreases so much that the  $p_z$  band, antisymmetric in the direction perpendicular to the ML, starts to be occupied and opens a new conduction channel. It is also interesting to note that the van Hove singularities lay close to the Fermi energy which, therefore, rises the DOS. All these interesting characteristics can only be explained in terms of the non-local character of the ionic pseudopotential [23].

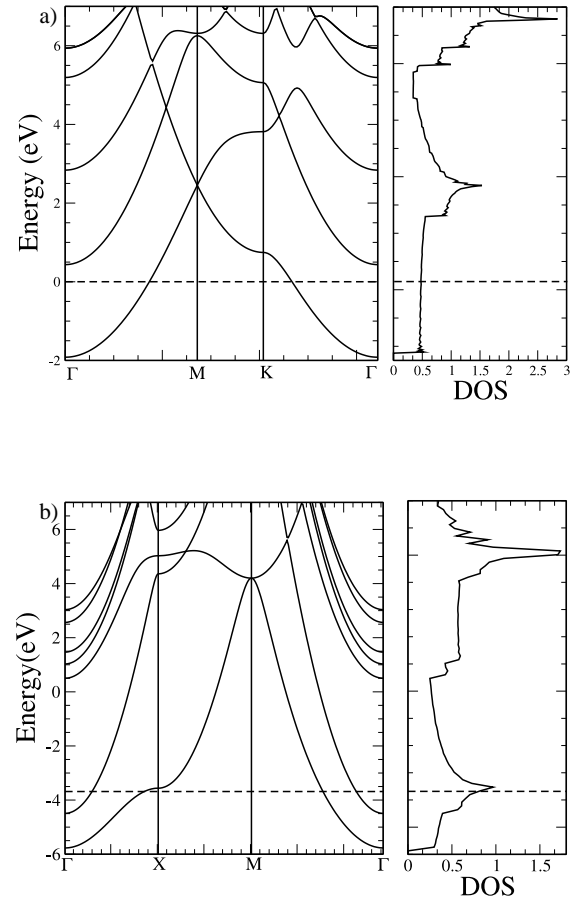


FIG. 2: Band structure and density of states (DOS) for (a) a hexagonal lithium ML at equilibrium ( $r_s = 3.02$  a.u.) and (b) a square structure with  $r_s = 2.15$  a.u. The Fermi energy is represented by the dotted line.

Another essential feature determining electronic properties of the ML is the geometry associated to the Fermi *line*, which is displayed in Fig. 3 for the same densities and structures as above. At equilibrium just one Fermi *line* exists, associated to the  $s$  band, which is almost circular as corresponds to a NFE approximation. However, as mentioned above, this simple picture breaks at higher densities. At  $r_s = 2.15$  a.u. there are two Fermi *lines* associated to the two occupied  $s$  and  $p_z$  bands and, surprisingly, the Fermi *line* associated to

the  $s$  band becomes a perfect square as corresponds to a half filled Hubbard-type model. As it is well known, this model becomes appropriate to describe electronic properties of systems with localized electronic states, just being the opposite case to the NFE approximation valid at normal pressures. The perfect nesting observed at  $r_s = 2.15$  a.u. strongly couples electronic states close to the Fermi *line* along the  $\overline{\Gamma M}$  direction, and might induce structural Peierls transitions.

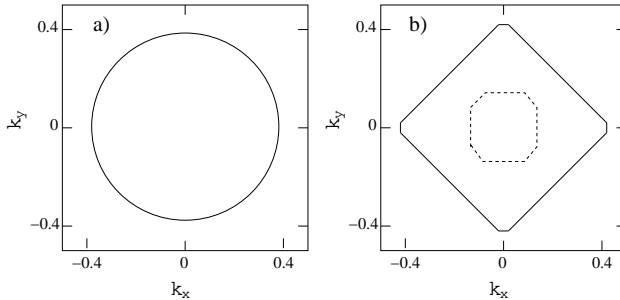


FIG. 3: Fermi *lines* of a) a hexagonal lithium ML at equilibrium and b) a square ML with  $r_s = 2.15$  a.u. The solid line corresponds to the Fermi *line* of the  $s$  band and the dotted line is associated to the  $p_z$  band, which becomes occupied at high densities.

## B. Peierls Transition

As a consequence of the nesting in the Fermi *line* at  $r_s \simeq 2.15$  a.u., any perturbation which breaks the electronic degeneration might be favored. Although different symmetry breaking perturbations might be proposed, in this section we have included the analysis of the two simplest diatomic square structures:  $dsq_1$  and  $dsq_2$ . In both structures we choose a diatomic square unit cell and allow the central atom to move along two highly symmetric directions: the nearest neighbor ( $dsq_1$ ) and second nearest neighbor ( $dsq_2$ ) directions.

In Fig. 4 we present the enthalpies as a function of the density for the five structures considered:  $hc$ ,  $hex$ ,  $sq$ ,  $dsq_1$  and  $dsq_2$ . It is interesting to note that at  $r_s \simeq 2.15$  a.u, just the density where the nesting in the Fermi *line* of the monoatomic square structure ( $sq$ ) is found, the new  $dsq_2$  structure proposed in this work is favored over the others. Therefore, the perturbation caused by the nesting in the Fermi *line* consists in a relative movement of the atoms in the second nearest neighbor direction, producing a charge density wave in this direction. However, at much higher densities ( $r_s = 1.35$  a.u.) the  $sq$  structure is favored again over the diatomic structures.

Fig. 5 shows the band structure and DOS for the  $dsq_2$  structure at  $r_s = 2.0$  a.u., which confirms the clear deviation from a NFE behavior, already manifested for

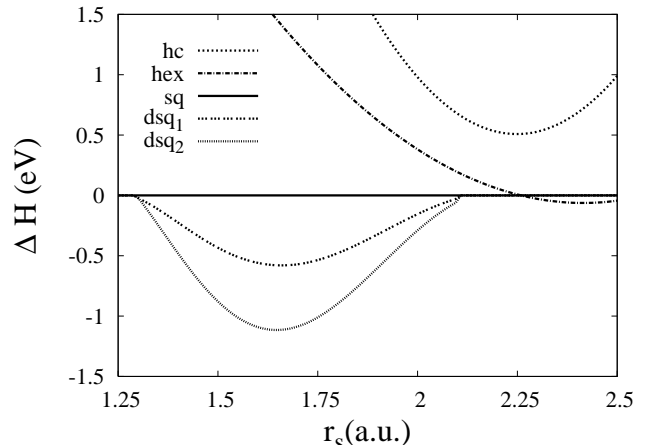


FIG. 4: Enthalpy as a function of the density parameter,  $r_s$ , for all the structures considered:  $hc$ ,  $hex$ ,  $sq$ ,  $dsq_1$  and  $dsq_2$ . All the enthalpies are referenced to the square enthalpy,  $\Delta H = H - H_{sq}$ . Although the  $sq$  structure becomes favored at  $r_s = 2.25$  a.u., the proposed new diatomic square structure ( $dsq_2$ ), where the atom at the center is allowed to move along the direction of the second nearest neighbor, is preferred at higher densities ( $1.3$  a.u.  $< r_s < 2.15$  a.u.).

the monoatomic structures of a lithium ML. The  $s$  band amazingly flattens in the  $\overline{XM}$  direction, which indicates a strong electronic localization in this direction, although the ML remains metallic. In Fig. 6 we plot the LDA valence charge density of the  $dsq_2$  structure at  $r_s = 2.0$  a.u. The charge density accumulates between the ions forming a clear one-dimensional conducting channel, which also originates a very sharp singularity in the electronic DOS close to the Fermi energy (Fig. 5).

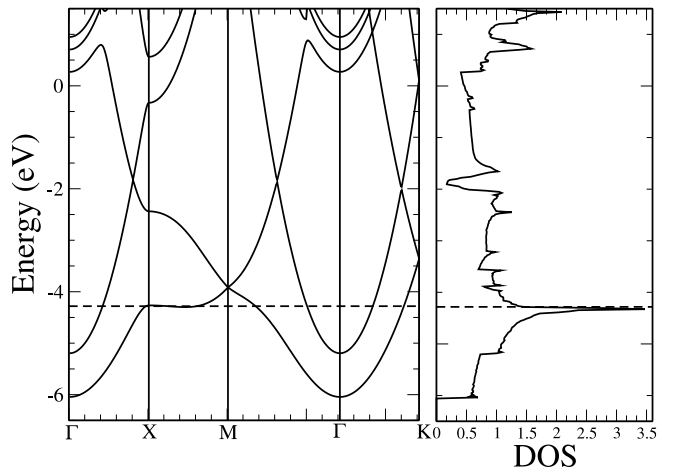


FIG. 5: Band structure and DOS of a lithium ML with  $dsq_2$  structure at  $r_s = 2.0$  a.u. The  $s$  band becomes extraordinary flat in the  $\overline{XM}$  direction.

In order to characterize the phase transition involving

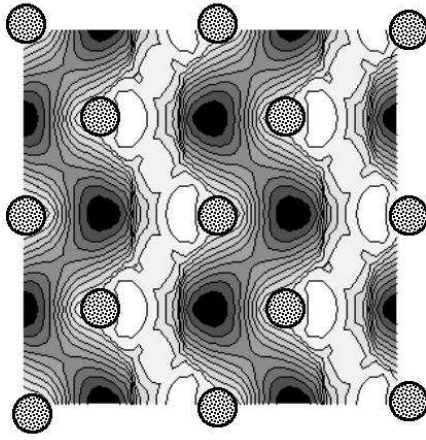


FIG. 6: LDA valence charge density of the proposed  $dsq_2$  lithium ML at  $r_s = 2.0$  a.u. The ions with core electrons are represented by circles with dots inside, while the valence charge density maximum (black areas) accumulates between them forming a clear one-dimensional conducting channel.

the  $dsq_2$  structure we have analyzed the displacement of the central atom along the minimum energy direction as a function of the density. As it is shown in Fig. 7 and expected from our analysis above, the atomic displacement is zero for  $r_s > 2.15$  a.u. However, at  $r_s = 2.15$  a.u. the high anharmonic potential of the central atom induces the presence of a soft phonon mode which moves the atom at the center. As it is displayed in Fig. 7, around  $r_s = 2.15$  a.u. the displacement of the central atom grows continuously with increasing density which indicates the second-order character of the  $sq \rightarrow dsq_2$  transition. However, if we keep rising the density, we find that at  $r_s \simeq 1.3$  a.u. the displacement of the central atom vanishes discontinuously and the ML goes back to the monoatomic  $sq$  structure. We have seen that this transition is explained by the presence of an absolute minimum energy at the center while relative minima at finite displacements from the center still remain, characterizing the  $dsq_2 \rightarrow sq$  transition as first-order.

### C. Magnetic Instability

In a low density electron gas it is well known that a ferromagnetic instability can be induced as the kinetic energy penalty in the ferromagnetic state is compensated by the gain associated to the electronic exchange [25]. So that, in principle, we would not expect such a transition to occur for high densities. However, as we can see in Figs. 2 and 5, the second band starts to be occupied as density

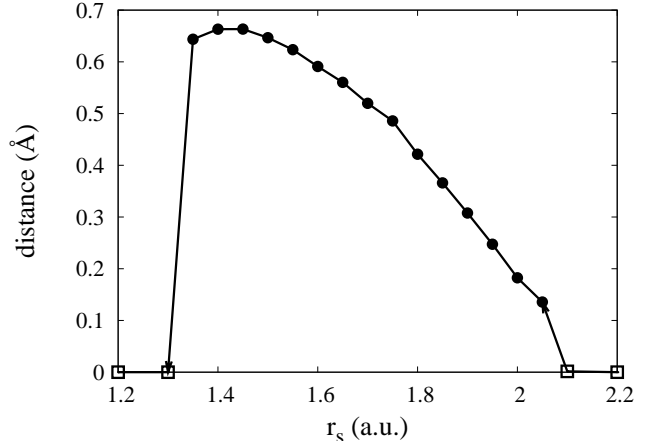


FIG. 7: Displacement of the central atom in the  $dsq_2$  structure (solid dots) along the second nearest neighbor direction as a function of the density. The open squares correspond to the  $sq$  structure, where the atom remains at the center.

is increased. Therefore, the effective low electronic density in the  $p_z$  band, in conjunction with the high DOS in the proximities of the Fermi energy and the nesting observed in the Fermi *line*, could induce a ferromagnetic instability in a lithium ML. Fig. 8 displays *ab initio* calculations within the LSDA approximation which predict that a ferromagnetic instability can occur in a narrow density range:  $2.2$  a.u.  $> r_s > 1.95$  a.u. It is interesting to notice that the maximum value of the net magnetic moment per conduction electron,  $\sim 0.14\mu_B$ , is observed at  $r_s = 2.1$  a.u, just at the density where the  $sq \rightarrow dsq_2$  Peierls structural transition takes place. This magnetic instability in a lithium ML, which has been shown to be correlated with electronic and structural transitions presented above, also proves the *complexity* that pressure induces in these, otherwise considered, *simple* systems.

## IV. CONCLUSIONS

In summary, according to the *ab initio* calculations presented in this work, although the NFE model correctly describes the properties of the lithium ML at normal conditions, it loses its validity as the electronic density increases. We have analyzed pressure induced *complexity* in structural, electronic and even magnetic properties of the ML, finding an interesting correlation between them. As density goes up, a flattening of the  $s$  band is observed, indicating an electronic localization. The corresponding nesting in the Fermi *line* and van Hove singularities in the proximities of the Fermi energy observed at  $r_s \simeq 2.1$  a.u. induce a Peierls second-order structural transition ( $sq \rightarrow dsq_2$ ). Beyond these features, at around the same density, the non-local character of the ionic pseudopotential allows to start filling the  $p_z$

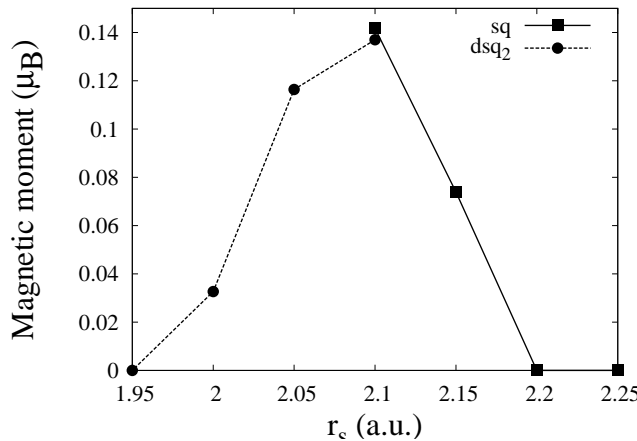


FIG. 8: Magnetic moment per atom as a function of the density,  $r_s$ , for a lithium ML with  $sq$  (squares) and  $dsq_2$  (dots) structures, which minimize the energy at the pressure range considered. Lithium ML presents a stable ferromagnetic ground state in the proximities of the Peierls transition, with a maximum net magnetic moment per atom of  $\sim 0.14\mu_B$ , located close to the density where the structural transition ( $sq \rightarrow dsq_2$ ) has been predicted,  $r_s = 2.1$  a.u.

band, and its low effective initial occupation causes a ferromagnetic Bloch instability. Besides of the intrinsic interest of studying the physical properties of systems with reduced dimensionality, the simplicity of the ML allows us to make a more detailed analysis and by extending these conclusions to bulk systems will provide us a very useful perspective to understand the physical origin of the *complexity* observed in compressed bulk lithium [26].

### Acknowledgments

A. Rodriguez-Prieto would like to acknowledge financial support from the Donostia International Physics Center (DIPC) and the Basque Hezkuntza, Unibertsitate eta Ikerketa Saila.

---

[1] E. Wigner and F. Seitz, Phys. Rev. **43**, 804 (1933).  
[2] J. B. Neaton and N. W. Ashcroft, Nature **400**, 141 (1999).  
[3] M. Hanfland, K. Syassen, N. E. Christensen, and D. L. Novikov, Nature **408**, 174 (2000).  
[4] J. B. Neaton and N. W. Ashcroft, Phys. Rev. Lett. **86**, 2830 (2001).  
[5] N. E. Christensen and D. L. Novikov, Solid State Commun. **119**, 477 (2001).  
[6] K. Shimizu, H. Ishikawa, D. Takao, T. Yagi, and K. Amaya, Nature **419**, 597 (2002).  
[7] V. V. Struzhkin, M. I. Eremets, W. Gan, H. K. Mao, and R. J. Hemley, Science **298**, 1213 (2002).  
[8] S. Deemyad and J. S. Schilling, Phys. Rev. Lett. **91**, 167001 (2003).  
[9] N. W. Ashcroft, Nature **419**, 569 (2002).  
[10] K. I. Juntunen and J. T. Tuoriniemi, Phys. Rev. Lett. **93**, 157201 (2004).  
[11] H. Uchida, D. Huang, F. Grey, and M. Aono, Phys. Rev. Lett. **70**, 2040 (1993).  
[12] C. T. Salling and M. G. Lagally, Science **265**, 502 (1994).  
[13] P. Hohenberg and W. Kohn, Phys. Rev. **136**, B864 (1964).  
[14] W. Kohn and L. J. Sham, Phys. Rev. **140**, A1133 (1965).  
[15] D. M. Ceperley and B. J. Alder, Phys. Rev. Lett. **45**, 566 (1980).  
[16] J. P. Perdew and A. Zunger, Phys. Rev. B **23**, 5048 (1981).  
[17] J. P. Perdew and Y. Wang, Phys. Rev. B **45**, 13244 (1992).  
[18] O. Gunnarsson and B. I. Lundqvist, Phys. Rev. B **13**, 4274 (1976).  
[19] G. Kresse and J. Hafner, Phys. Rev. B **47**, 558 (1993).  
[20] G. Kresse and J. Furthmüller, Phys. Rev. B **54**, 11169 (1996).  
[21] P. E. Blöchl, Phys. Rev. B **50**, 17953 (1994).  
[22] H. J. Monkhorst and J. D. Pack, Phys. Rev. B **13**, 5188 (1976).  
[23] A. Bergara, J. B. Neaton, and N. W. Ashcroft, Phys. Rev. B **62**, 8494 (2000).  
[24]  $r_s$  is the two-dimensional linear density parameter, defined by the relation  $A/N = \pi(r_s a_0)^2$  where  $N$  is the number of nuclei in a ML with area  $A$  and  $a_0$  is the Bohr radius.  
[25] F. Bloch, Z. Physik **57**, 545 (1929).  
[26] A. Rodriguez-Prieto and A. Bergara, to be published.